14625

Thermal Runaway

Henry A. Catherino
U.S. Army Research Development and Engineering Command
AMSRD-TAR-R/MS 121
Warren, MI 49397-5000
catherih@tacom.army.mil

Abstract

During battery discharge, the heat generated is the sum of the Joule (resistive) and enthalpic (chemical) heating effects. Conversely, during battery charging, the heat generated is the Joule minus the enthalpic heating. If the conditions are carefully selected, one can observe a net battery cooling during charging.

However, an interesting phenomenon takes place during overcharge. Those cells designed as sealed recombinant systems develop significant heating. Flooded designs do not exhibit this effect. The applied electric power generates energetic reaction products as a consequence of the electrochemical reactions. This is an energy absorbing process. The gasses are then vented into the environment. Since the sealed cells undergo a closed recombination cycle, i.e., no material is exchanged with the environment, the rate of heat generated is proportional to the power input to the cell. Essentially, the cell is behaving in the manner of a resistor.

In this connection, the thermal runaway phenomenon that has been often observed in starved electrolyte cell designs raises a potential problem in battery applications.

It is not efficient to design around the worst case scenario, i.e., anticipating the thermal runaway effect. It is wiser to detect its onset and shut down the charging process. An alternative approach is to develop an understanding of the Thermal Runaway process and, perhaps, develop a method for eliminating or effectively controlling it.

A study was performed in attempt to model the thermal runaway effect. In short, the effect appears to be related to the electrolyte distribution in the separator. This suggests that modification of the AGM separator properties could provide a means for better controlling the thermal runaway failure mode.

Introduction

Thermal runaway is a prevalent failure mode appearing in recombinant lead acid batteries [1]. On occasion, VRLA batteries are removed from service because the battery gets quite hot to the touch during constant voltage charging. This heating has often been attributed to the exothermic recombination of oxygen at negative electrodes. Under normal conditions, constant voltage charging of lead acid batteries shows a decrease in current approaching an asymptotic limit. In the case of the thermal runaway, the current

Report Documentation Page

Form Approved
OMB No. 0704-0188

1. REPORT DATE	2. REPORT TYPE	3. DATES COVERED
21 FEB 2005	**N/A**	**-**

4. TITLE AND SUBTITLE	5a. CONTRACT NUMBER
Thermal Runaway	5b. GRANT NUMBER
	5c. PROGRAM ELEMENT NUMBER
6. AUTHOR(S)	5d. PROJECT NUMBER
Henry A. Catherino	5e. TASK NUMBER
	5f. WORK UNIT NUMBER
7. PERFORMING ORGANIZATION NAME(S) AND ADDRESS(ES)	8. PERFORMING ORGANIZATION REPORT NUMBER
USA TACOM 6501 E 11 Mile Road Warren, MI 48397-5000	**14625**
9. SPONSORING/MONITORING AGENCY NAME(S) AND ADDRESS(ES)	10. SPONSOR/MONITOR'S ACRONYM(S)
	TACOM TARDEC
	11. SPONSOR/MONITOR'S REPORT NUMBER(S)

12. DISTRIBUTION/AVAILABILITY STATEMENT
Approved for public release, distribution unlimited

13. SUPPLEMENTARY NOTES

14. ABSTRACT

15. SUBJECT TERMS

16. SECURITY CLASSIFICATION OF:			17. LIMITATION OF ABSTRACT	18. NUMBER OF PAGES	19a. NAME OF RESPONSIBLE PERSON
a. REPORT	b. ABSTRACT	c. THIS PAGE			
unclassified	**unclassified**	**unclassified**	**SAR**	**23**	

Standard Form 298 (Rev. 8-98)
Prescribed by ANSI Std Z39-18

can rise to the power supply's current limit. Figure 1 shows a normal charging curve for a VRLA battery. The early constant current portion is the consequence of the power limitation of the power supply used to charge this battery. The declining portion of the curve is the consequence of the increasing battery voltage resulting from the increasing state of charge of the battery. The current eventually reaches an asymptotic limit where small internal parasitic processes sustain a very low current flow.

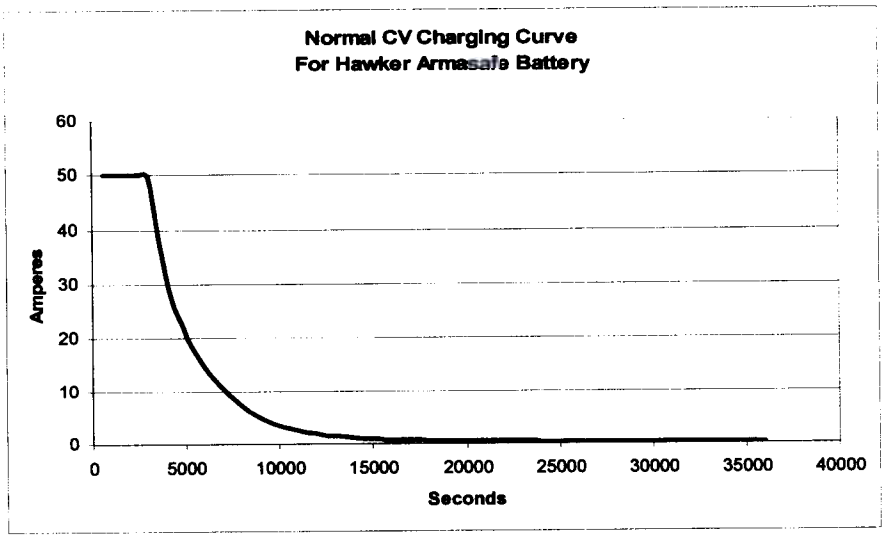

Fig. 1. Normal constant voltage charging curve for battery.

In contrast, Figure 2 shows the battery's response during thermal runaway observed while the battery was being charged under normal constant voltage charging conditions.

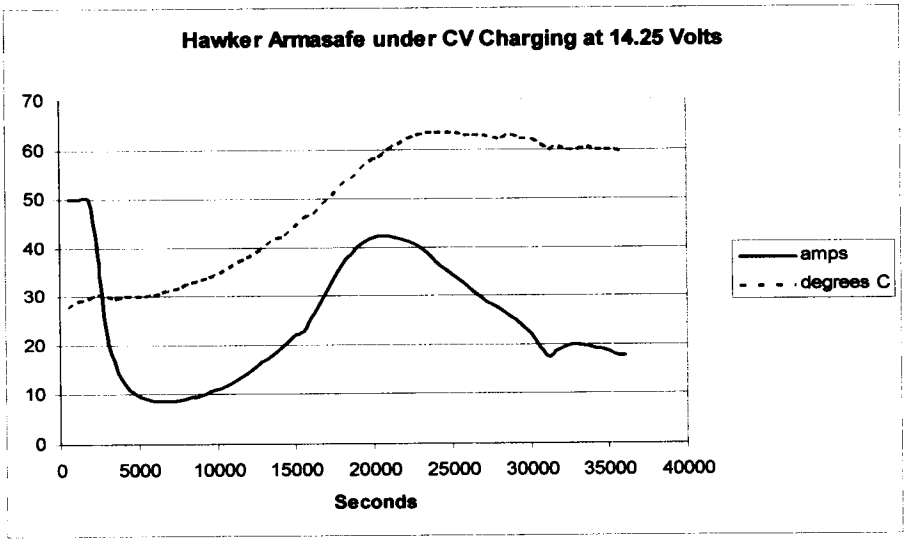

Fig. 2. Current and temperature response of a VRLA battery in Thermal Runaway.

When this failure mode appears, the effect is very evident and is easily identified. An examination of this failure mode has value in order to understand why it occurs and by doing that, to determine ways of minimizing its occurrence.

Experimental Note

The author is aware of two methods for inducing the thermal runaway of a VRLA battery in the laboratory. Application of these methods provides a means of accelerating the thermal runaway effect for the purpose of study. The first and quickest way to induce the effect is to charge a VRLA battery well above its recommended charging voltage. For example, a VRLA battery designed for a nominal 12V operation could be charged at 16V to induce the effect. The second method takes a little longer to bring about the effect. Specifically, a VRLA battery is cycled using a constant current during both charge and discharge. The charging takes place at about a C/2 rate until the temperature at the negative terminal rises to a maximum of 40 degrees Celsius. The subsequent discharge can be carried out a C/10 rate to an appropriate cutoff voltage (i.e., 10.5V for a 12 volt nominal battery). Repeating this for 50 cycles and then initiating a standard constant voltage charge to the battery from a discharged state has resulted in a thermal runaway. In the study here, this was the preferred method. The repetitive cycling serves to precondition the battery to make it susceptible to thermal runaway. The desired objective was to demonstrate the effect as it would take place under "normal" operating conditions. This methodology may most closely represent what appears when the thermal runaway failure takes place under normal applications. Of course, the usual caveats must be kept in mind whenever one uses accelerated testing methods to induce a failure mode. Also, the methods described above have not been optimized to induce any particular result. In the tests performed, the rated capacity of the batteries was nominally 120Ah. The discussion that follows attempts to give an interpretation to the variety of behaviors observed during thermal runaway as observed using the induction procedure described.

Discussion

The phenomenon of thermal runaway was discussed by D. Pavlov as a consequence of the closed oxygen cycle in valve regulated lead acid batteries [2]. Essentially, during the charging of a VRLA battery and starting at about 70% state of charge, oxygen begins to evolve at the positive electrode at very low rates. The design of the battery provides an efficient means for removing the oxygen by recombination at the negative electrode. This charging process normally takes place at constant applied voltage. The observed charging current decreases exponentially and approaches a low steady state value. This low limiting current is indicative of the completion of the charging. The oxygen recombination process continues at a very low rate at the applied charging voltage. This is the normal behavior observed during the battery charging.

Pavlov presented a critical insight into the thermal runaway effect. The interpretation is based on an observation made by Pavlov and Monahov [3]. Essentially, the normally operating VRLA battery is a closed system. In the closed system, the rate of the oxygen

recombination at the negative electrode is determined by the rate of oxygen evolution at the positive electrode. The oxygen generation rate is dependent on the potential and the temperature at the interface of the positive electrode. Reproduced here is a Tafel plot showing the critical dependencies of the electrochemical oxygen evolution on the PbO_2 layer on the positive electrode at various measured cell temperatures. The experimental data is shown in Fig. 3.

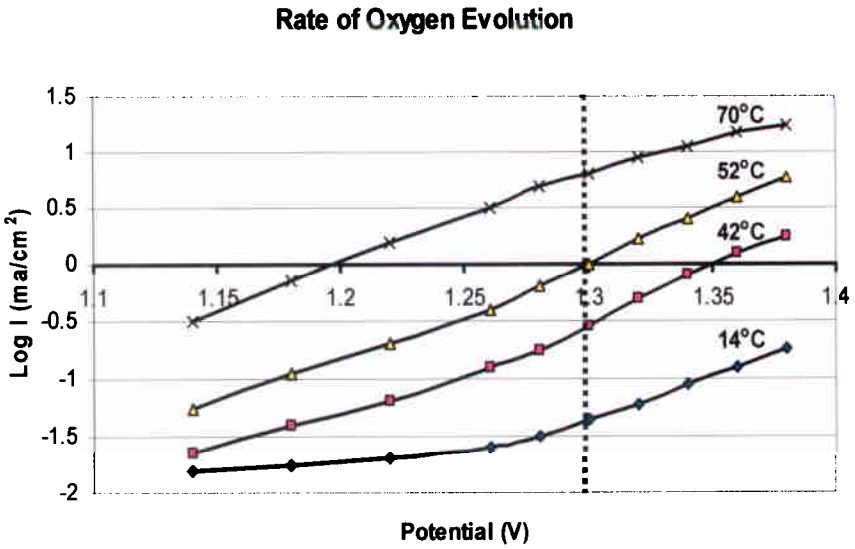

Fig. 3. Tafel dependencies of the oxygen electrode at different temperatures. The potential of the oxygen electrode is measured versus a Hg/Hg_2SO_4 reference electrode.

The influence of temperature can be seen by holding the electrode potential constant and observing the rate of the oxygen evolution reaction which is proportional to the log of the measured current density. As shown in the figure, by holding the electrode potential equal to 1.3 V versus a $Hg/HgSO_4$ reference electrode, the currents at the different temperatures can be identified. For example, at 42 °C the current density passing through the electrode is 0.26 A/cm^2 as compared to 1.072 A/cm^2 at 52 °C. This is showing that a 10 °C temperature increase is causing a four-fold increase in the rate of oxygen evolution. This is a characteristic Arrhenius temperature dependence on rate processes:

$$\text{Rate} = k\, e^{-\Delta H/RT}$$

The approach to the mechanistic interpretation discussed below is based on observing the exponential dependence of the oxygen evolution reaction on temperature while holding the electrode potential constant.

Heat Management Discussion

To begin to analyze this complex process, it is helpful to consider the situation where a fixed current acts to generate oxygen that recombines at the negative electrode. A sealed system is assumed. The heat thus generated establishes a steady state with the heat

removal process. To simplify the description of the modeled process, it is convenient to assume that the charging component associated with energy storage is complete so that the heat production is represented as coming from Joule heating and the enthalpy of reaction of the oxygen recombination process. The heat removal process is given in its usual form as being proportional to the temperature gradient between the source and the environment.

Rate of Joule Heating + Enthalpic Heating = Rate of Heat removal

$$(IEoc + I_2R_{Polarization}) + ke^{k'T} = m(T-T_0)$$

In this formulation, the Joule component is given by the sum of two terms. IEoc is the applied current multiplied by the open circuit voltage of the battery. The second term is the Joule contribution from the polarization resulting from the applied current. It is to be noted that the magnitude of the current which is proportional to the rate of oxygen production is in turn equal to the rate of oxygen recombination. That is the steady state requirement. Also:

$$IEoc >> I^2R_{Polarization} \quad \text{and} \quad I = Ke^{k'T}$$

then, substituting:

$$(Ke^{k''T})\,Eoc + ke^{k'T} = m(T-T_0)$$

or

$$k_1e^{k''T} + k_2e^{k'T} = m(T-T_0)$$

At this point, it is instructive to ask which term on the left hand side of the previous equation is larger. That is, is it the Joule heating or the chemical enthalpy that predominates? A prevalent view is that the recombination of oxygen is said to be the major source of the heat generation during overcharge.

It is important to emphasize that a position will be taken here that is contrary to that view point. That is, in the closed oxygen cycle, the net enthalpy of the reaction is zero. The closed oxygen cycle contributes no heat to the overcharge process. It is to be understood that the meaning of a "closed cycle" infers that no material leaves the battery and that the reactants and products return to their original state. In that case, the enthalpy of the cyclic process is necessarily zero.

Although this observation is nothing more than a requirement placed on the system by the energy conservation law, a few additional comments are in order because this conclusion stands in opposition to some widely held views on the subject. Specifically, it is a commonly held view that the oxygen recombination step that is the heat generating mechanism taking place during overcharge in a sealed battery system. It is also worth

noting that various authors have taken guarded positions on this admitting only that a correlation exists between the oxygen recombination process and the heat generation effect. The "leap of faith" takes place as the result of the well-established observation that the reaction of oxygen with metals is known to be exothermic.

To support the position taken in this exposition, consider the following reactions as representing a Closed Cycle Process: (One can add more complexity if desired but this keeps it simple.)

During overcharge:

- At the negative electrode $2Pb + O_2 \rightarrow 2PbO$
  $PbO + 2H^+ + 2e^- \rightarrow H_2O + Pb$ (2X)
- At the positive electrode $2H_2O \rightarrow O_2 + 4H^+ + 4e^-$

Then this sequence of processes can be represented as a Born – Haber Cycle. Using this sequence of reactions as an example:

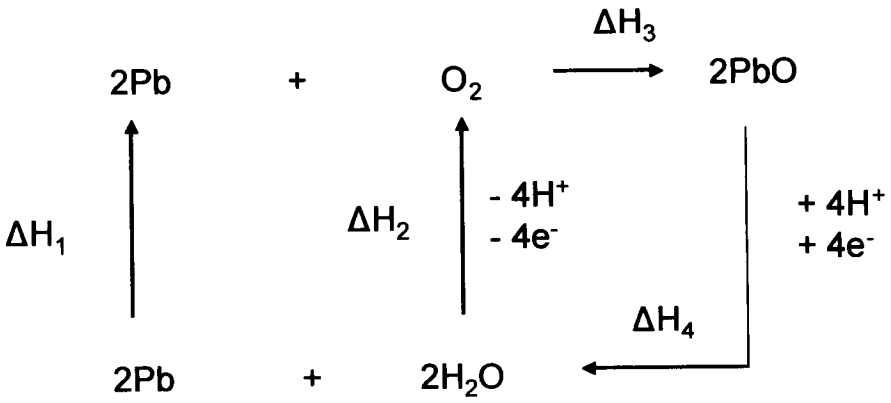

Fig. 4. Born-Haber Cycle illustrating the essential parts of the Closed Oxygen Cycle.

This cycle illustrates a sequence of the states of matter corresponding to the chemical changes occurring during the cycle. To illustrate the application of this cycle, the following exercise is presented.

$\Delta H_1 + \Delta H_2 + \Delta H_3 + \Delta H_4 = 0$ The First Law of Thermodynamics

$\Delta H_1 = 0$ No change of state takes place

$\Delta H_2 = +571.88$ kJ/mol O_2 (Pavlov [2])

$\Delta H_3 = -(2)(195.2)$ kJ/mol Pb (Standard Heat of Formation of PbO)

ΔH_4 = Quantity to be determined

Then:

$$\Delta H_4 = [0 - 571.7 + (2)(195.2)]/2 \quad \text{kJ/mol PbO} = 90.65 \text{ kJ/mol PbO}$$

for the reaction:

$$PbO + 2H^+ + 2e^- \rightarrow H_2O + Pb$$

The point is that the sum of all the enthalpies associated with each of the participating reactions occurring in a closed cycle must equal zero. Otherwise one can create or destroy energy depending on the direction one moves around the cycle.

As applied to the Closed Oxygen Cycle, the claim that no net heat is generated is a theoretically based argument. No empirical data is presented here to support it. It is noteworthy that the position taken in this discussion involves a different paradigm. That is, either energy is conserved or it is not conserved. The position taken is based on first principles and not on experimental data. There is an interesting philosophical issue involved.

As a summary, the exothermic heat of recombination of oxygen at the negative electrode is acknowledged. However, all of the reactions taking place in the electrode pack have to be considered. The sum of the heats of reaction of each of the steps leading to the recombination and regenerating the reactants is the enthalpic component. In that case, the closed cycle necessarily requires that no net heat can be generated. If this is taken to be the case, then the only source of heat produced during the overcharge is the Joule heating contribution.

For the discussion that follows, it is only necessary to observe that the heat production rate is an exponential function and the heat removal process is a linear function.

It is the behavior of the mathematical functions in the steady state relationship that is instructive. Figure 4 shows a functional response for the purpose of showing the steady state condition:

$$k\, e^T = m\,(T-T_0)$$

Figure 5 plots the exponential rate of heat generation and the linear rate of heat removal. In this plot, m was assigned a value of 5, k the value of 1 and T_0 the value of 0. These values are taken as a matter of convenience. It is not the specific values that are of importance here. The emphasis is being place on the dynamical response of the mathematical functions.

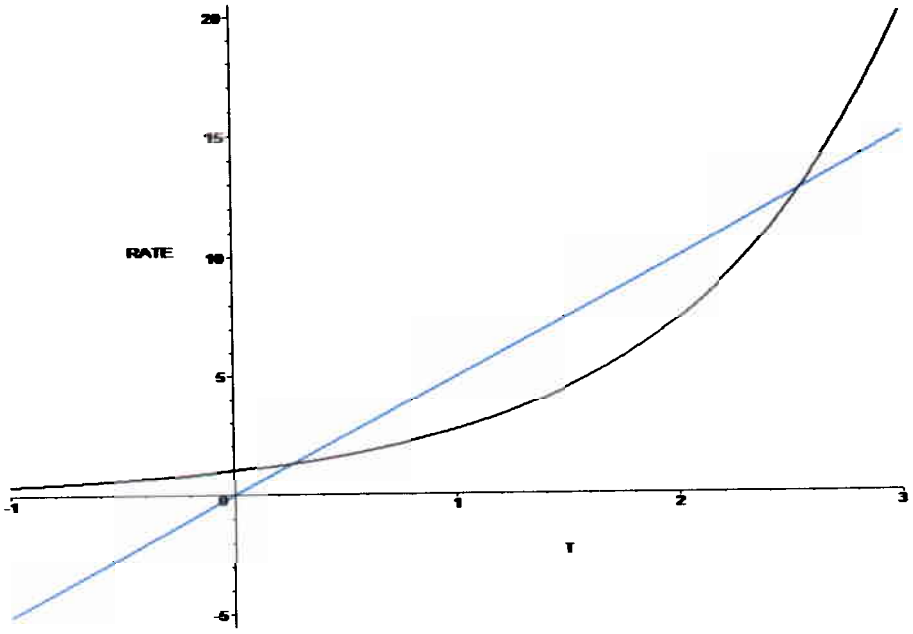

Fig. 5. A plot of the linear heat transfer process and the exponential Arrhenius function.

In this plot, two points of intersection are shown. These intersection points correspond to the possible steady state conditions that can exist. That is, the states where the rate of heat generation equals the rate of heat removal.

In passing it is necessary to mention that three possible conditions can exist. First, the slope of the linear function can be small enough such that the linear function does not intersect the exponential curve. In that case no steady state exists. This means that the system response would rise without bound. This situation is not relevant to the case under consideration. Second, the slope of the linear function can be tangent to the exponential curve. This is actually a special case where two intersection points converge into one point. The third case is the situation shown where two intersection points exist.

Discrete Dynamical Modeling

To analyze this situation, an approach based on discrete dynamical modeling will be used [4]. To do this, the steady state expression shall be rewritten as:

$$\ln(k) + T_n = \ln(m) + \ln(T_{n+1} - T_0)$$

or

$$T_{n+1} = [k \exp(T_n) + mT_0]/m$$

From the previously assumed values of m, k and T_0, the following difference equation results:

$$T_{n+1} = \exp(T_n)/5$$

It is now possible to analyze the response of the system at points other than the two intersection or equilibrium points.

Difference Analysis

The analysis begins by assigning a value to T as the initial value. This value determines the rate of heat generation. From this assignment, the value of T necessary to transfer the heat generated to the environment at the rate at which it was produced is determined. Figure 5 show the consequence of assigning an initial value of T that is between the two intersection points (i.e., equilibrium points). This diagram is sometimes called a cobweb analysis. The consequence of this calculation is that the T is driven downward to the intersection point at the lower value of T. The figure illustrates this effect.

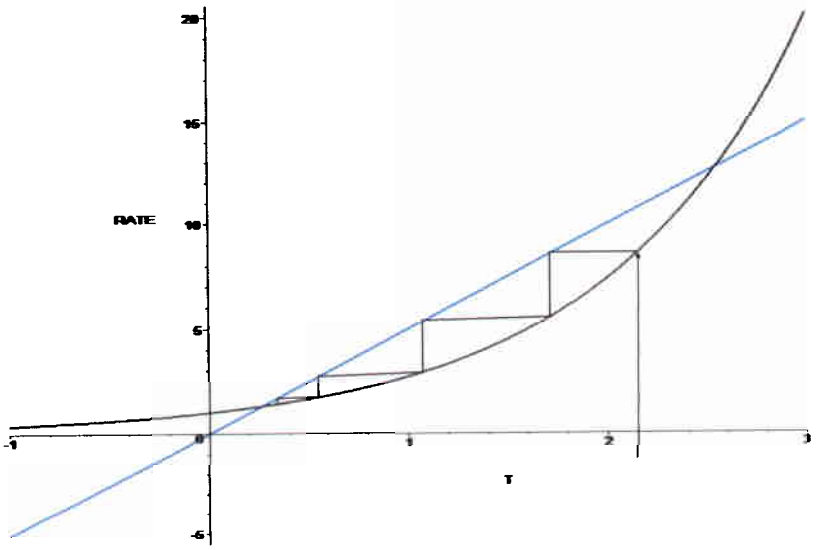

Fig. 6. A Cobweb Diagram showing the sequential steps as they approach the equilibrium point.

The actual iterative calculation is shown in Figure 6 showing the convergence to the equilibrium point.

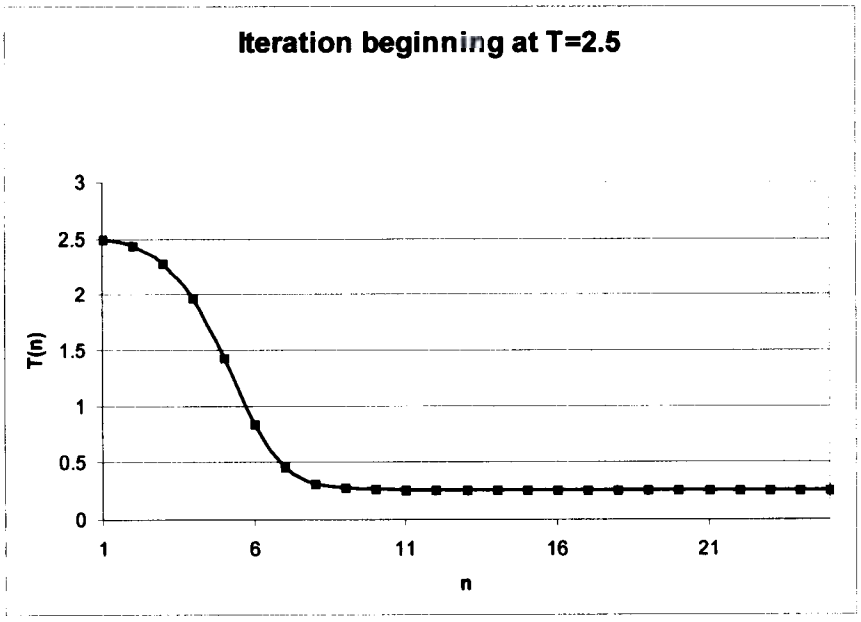

Fig. 7. Plot of the calculated points as the system approaches the equilibrium point brom above.

The convergence take place at about T= 0.259. The same analysis can assume that the initial value is set below the lower convergence point. If one assigns the initial value of T as 0.1, the consequence is shown in Figure 7. This time the rate of heat removal obligates the temperature for heat removal to rise until the convergence point is reached.

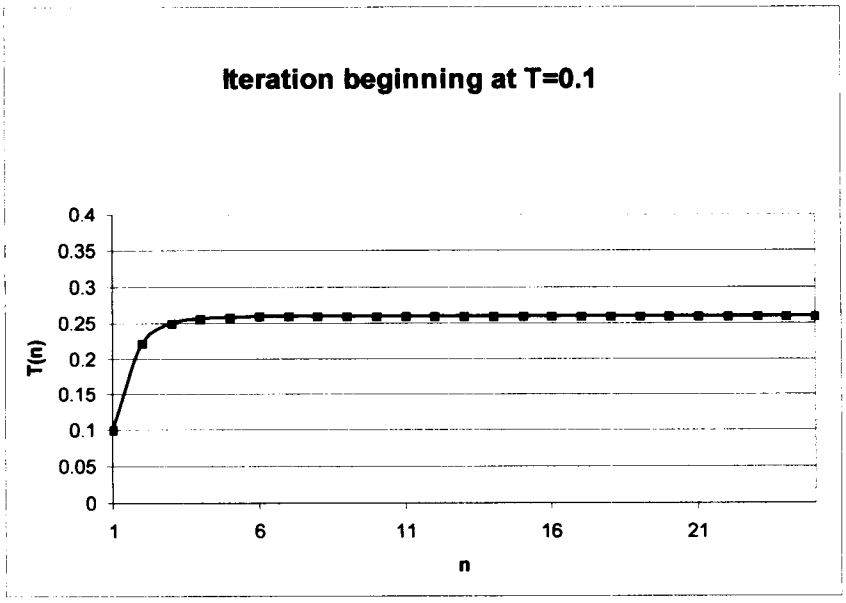

Fig. 8. Plot of the calculated points as the system approaches the equilibrium point from below

Finally, an initial value of T is chosen which higher than the upper equilibrium point the result is shown in Figure 8.

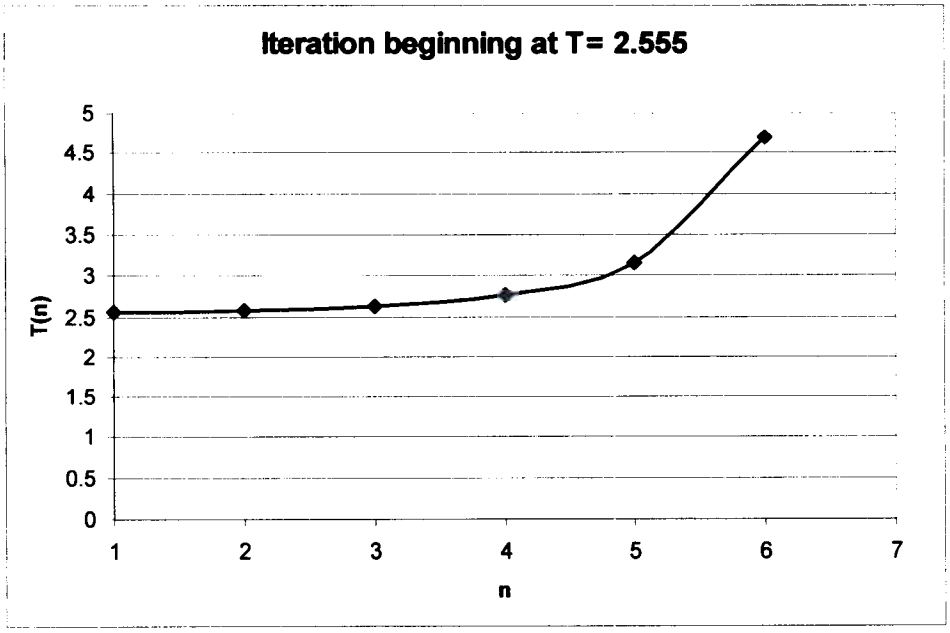

Fig. 9. Plot of the calculated points as the system deviates starting above the upper equilibrium point.

The starting value has to be selected near and above the equilibrium point to see that T diverges. The value of T then rises without bound.

From this it is evident that the two equilibrium points have different properties. The lower valued equilibrium point is a fixed point attractor. The upper point is often called a saddle point attractor. If one can achieve the exact equilibrium value of T, the equilibrium could be stable. An analogous occurrence takes place at the two equilibrium points of a pendulum. The point directly below the fulcrum is a fixed point attractor. The equilibrium point directly above the fulcrum is a saddle point attractor. That is, it is an unstable equilibrium point.

Having analyzed the behavior of the functional response of the controlling equations, an interpretation of the behavior of thermal runaway can be given.

Discussion of Thermal Runaway using this modeling approach

When the battery is being charged and oxygen evolution begins, the electrode pack begins to heat up. As the heating begins, the system behaves adiabatically. Shortly afterwards, the heat removal process begins. The rate of the heat removal acts to lower the temperature within the electrode pack. From the previous discussion, the maximum

temperature reached within the electrode pack becomes very important. If the temperature never exceeds the saddle point attractor temperature, the system will eventually drop to the lower steady state equilibrium point. However, should the transient temperature rise exceed the saddle point attractor temperature, the heat transfer process cannot remove heat faster than the charging current can generate it. A thermal runaway condition exists.

Without attempting to quantify the actual temperature for this cross over point, it is instructive to consider the factors that can induce a high initial electrode pack temperature and the factors affecting the curve intersection giving the saddle point.

Factors controlling the heat capacity of the electrode pack.

The following analysis can be found in paper by Pavlov [2] for a particular battery. The weights of the electrode pack components (the active block) are distributed as shown in Table 1. Table 2 lists the heat capacities of those components.

Table 1. Weights of active block components

	Unit weight m(g)	Number per cell	Total Weight
Positive grid	80	5	400
Negative grid	50	6	300
PAM	120	5	600
NAM	85	6	510
H_2SO_4, sp.gr. 1.28			680
AGM			50

Table 2. Specific heat capacities

	C (cal/g K)		C (cal/g K)
Pb	0.0305	H_2O	1
PbO_2	0.0646	H_2SO_4 (sp.gr. 1.28)	0.676
H_2SO_4	0.339	glass	0.15

Calculating the contribution of the different component to the net heat capacity, it can be shown that the electrolyte solution contributes as much as 85% of the active block heat

capacity. It follows that small changes in the electrolyte quantity can significantly affect the heat capacity of the electrode pack.

Also, it necessarily follows that the loss of water in the electrode pack can affect the adiabatic response of the system. By reducing the water content, an applied current can cause an exaggerated temperature excursion by virtue of the decrease in the heat capacity of the adiabatic system.

Reducing the thermal resistance of the electrode pack

In addition, the slope of the curve corresponding to the rate of heat removal depends on the heat transfer coefficient is proportional to surface area. The proportionality constant is sometimes called the thermal resistance. Its value depends on the insulative properties of the material. It one want to reduce the saddle point intersection point, the value of the heat transfer coefficient would be reduced. One way of doing that is to increase the number of dead gas spaces within the electrode pack. That is most easily accomplished by removing water from the electrode pack.

There is a common factor affecting the thermal runaway effect. The effect of water loss affects thermal runaway by virtue of (a) enhancing the transient thermal response and (b) reducing the steady state temperatures where the rates of generation and removal are equal.

On the Mechanism of the Thermal Runaway Process

Based on the preceding discussion, the following mechanistic interpretation can be offered (see Figure 10).

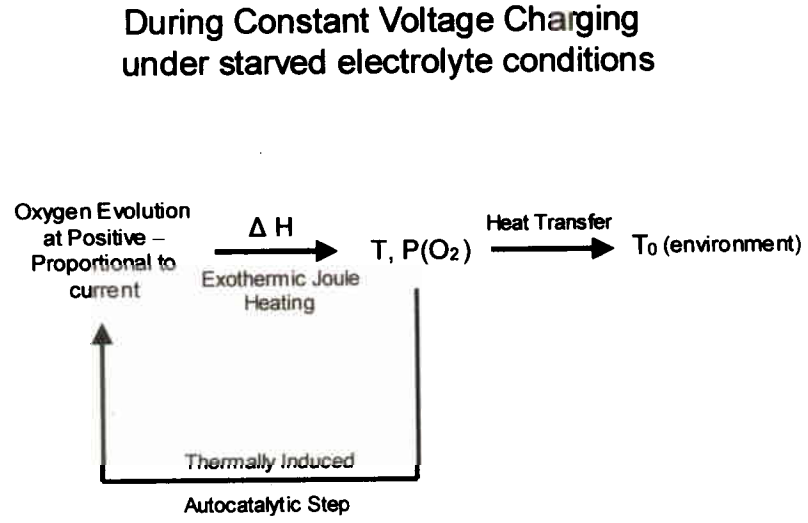

Fig.10. A representation of the essential steps in thermal runaway.

During a normal constant voltage charging of a battery as one approaches the end of the charging process, part of the applied current causes oxygen to be evolved. Also, during overcharge, the entire current is converted to oxygen production. The following mechanistic steps follow.

The water is electrolyzed absorbing storing energy, oxygen recombines at the negative electrodes generating heat and the Joule heating occurs by virtue of the current flow. A steady state temperature is eventually established between the rates of heat generation and heat removal. Also, a steady state partial pressure is achieved between the rates of oxygen evolution and recombination. The rise in temperature results in an autocatalysis raising the rate oxygen evolution together with an increased cell current flow and that in turn produces more heat. Also, the increased temperature increases the rate of heat removal.

The preceding discussion describes the situation induced by a transient thermal response. That is, should the initial temperature rise climb to level where the rate of heat removal is insufficient to remove the heat, then the autocatalysis forces the reaction to proceed at an ever increasing rate.

Of course this process cannot raise the temperature indefinitely. Another process will occur to limit the temperature rise. One possibility is that the excessive oxygen pressure might vent from the battery. Another possibility is that the electrolyte might boil and remove energy via a liquid to gas phase transition.

The preceding gives a picture of a complex mechanism that allows inferences to be made. These inferences permit the proposed mechanistic hypothesis to be tested.

At this point in the exposition, it is helpful to return to the observation made earlier. Fig. 2 showed an interesting attribute that took place during the charging process when the battery was in thermal runaway. Over a period of time, the temperature of the battery remained essentially constant while the applied current decreased. This constant temperature indicates that a steady state exists between the rate of heat generation and heat removal. The following is an attempt to rationalize this in view of the observed decreasing current. To do this, the model assuming only Joule heating shall be invoked. In that case the rate of heat generation is constant so:

$$I^2R = k_1 \text{ (steady state condition)}$$

In this case, the value of R is not the polarization resistance. It is to be understood as the effective resistance determined as if the battery were dissipating heat as an ordinary resistor. A resistor can be physically analyzed as:

$$R = \rho\, l/A = k_2 /A \quad \text{(at constant T)}$$

where ρ is the resistivity, l is the length of the resistive path and A is the cross-sectional area. The resistivity and the path length are held constant by the geometry of the battery. By rearranging and lumping the constants together,

$$I^2 k_2 / A = k_1$$

$$I^2 = k_3 A$$

$$I = k_4 \sqrt{A}$$

The inference here is that if the cross-sectional area of the resistor changes such that the current is proportional to the square root of the cross-sectional area, a constant rate of heat generation takes place. This situation can conceivably take place when the electrolyte in the intercell gap is being displaced by the generation of gas. This hypothesis is interesting because water is being moved from the intercell pack but not from the cell enclosure. This provides a slightly modified interpretation of the interpretation given by Pavlov [2]. Indeed, the low water loss from the battery observed as a consequence of the thermal runaway can now be reconciled with the changes of the heat capacity of the cell pack cause by water loss. That is, it appears that electrolyte is being "pumped" out of the inter-electrode gap by the gas evolution process.

The mechanistic hypothesis is adequate for further testing. The hypothesis allows for designing experiments for verification and provides a means for making performance predictions.

Carrying the Analysis Further

The low water loss and the presence of thermal runaway suggest that the increased resistance is the consequence of electrolyte displacement from within the interelectrode gap.

Note that an increased interelectrode resistance caused by electrolyte movement leads to an interesting speculation. Electrolyte movement:

(1) increases the IR drop in the intercell gap;
(2) by holding constant battery voltage, this decreases the oxygen electrode potential;
(3) this reduced potential decreases the rate of the oxygen gas evolution reaction;
(4) this in turn allows the electrolyte to flow back into the interelectrode gap;
(5) the consequence of this is a decrease in the cell resistance;
(6) the rate of gas evolution increases displacing more electrolyte;
(7) and the IR drop in the cell increases again.

It would follow that by maintaining a constant applied voltage, an oscillating current is a possible consequence. This effect has been previously observed.

Setting up Dynamical System for Analysis

From the preceding description, a dynamical model can be generated by, again, studying the response of the mathematical functions. During overcharge the applied voltage can be written as:

$$V(cell) = E(Pb) + E(O_2) + IR$$

Solving for the oxygen electrode potential gives:

$$E(O_2) = V(cell) - E(Pb) - IR$$

Since:

(a) V(cell) is a constant applied voltage
(b) E(Pb) is depolarized by O_2 recombination

then

$$E(O_2) = k_1 - IR$$

and

$$\text{Rate of reaction} = k_2 \exp k_3(E(O_2))$$

Substituting

$$\text{Rate of reaction} = k_2 \exp k_4(-IR)$$

Next, let $IR = \rho T$ where ρ shall be considered a coupling constant. The general properties of this coupling are that ρ is small in an environment where the electrolyte easily flows back into replace the gas bubbles produced such as in a flooded system and large in the case where it is difficult to displace the gas bubbles such as in a immobilized electrolyte condition. Then

$$i \text{ (rate of reaction)} = k_2 \exp k_4(-\rho T) \qquad \text{Oxygen Electrode (1)}$$

and

$$i \text{ (rate of reaction)} = k_5 \exp k_6 T \qquad \text{Arrhenius Component (2)}$$

These equations illustrate the competing processes of the accelerating effect of the Arrhenius response and the retarding effect of the decreased polarization caused by the iR drop.

By setting up the analysis graphically as a discrete dynamical model, some inferences can be made about the system behavior based on this model. The first case shall assume that a weak coupling takes place between the thermally catalyzed gas production and the ability of the electrolyte to return into the intercell gap to reduce the IR drop. The IR drop reduction serves to reduce the retarding influence on the electrode potential driven oxygen evolution reaction.

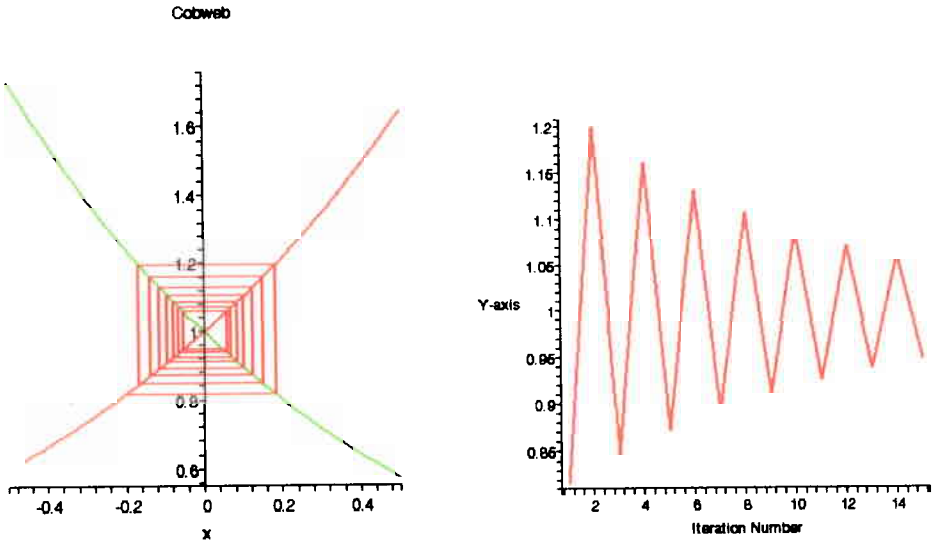

Fig. 11. X-axis is a function of T and the Y-axis is a measure of the reaction rate
$\rho \sim$ weak coupling

The abscissa (the x-axis) is proportional to the temperature and the ordinate (y-axis) is proportional to the rate of the reaction (or applied current). The iteration represents initially the effect of temperature on the temperature catalyzed reaction rate. To sustain that that rate, the IR drop required to do this would have to rise. That is, IR is determined by the coupling constant. At this temperature, the thermally catalyzed process would increase the rate of reaction (i.e., the gas generation). To sustain that rate, the IR drop would have to drop corresponding to a lower temperature. This repetitive sequence of events is seen to converge to an equilibrium point (an attractor). Fig. 11 illustrates that the equilibrium point is stable and the convergence can take place even more quickly as the coupling becomes weaker.

In the case of a strong coupling condition, the equilibrium point is unstable (a saddle point attractor). Fig. 12 shows that the temperature excursions exhibit a reinforced oscillation that grows without bound. Clearly, this suggests that some other process would intervene so as to eventually limit the temperature growth.

Figure 13 shows an intermediate condition which is the transition between a stable and unstable equilibrium point.

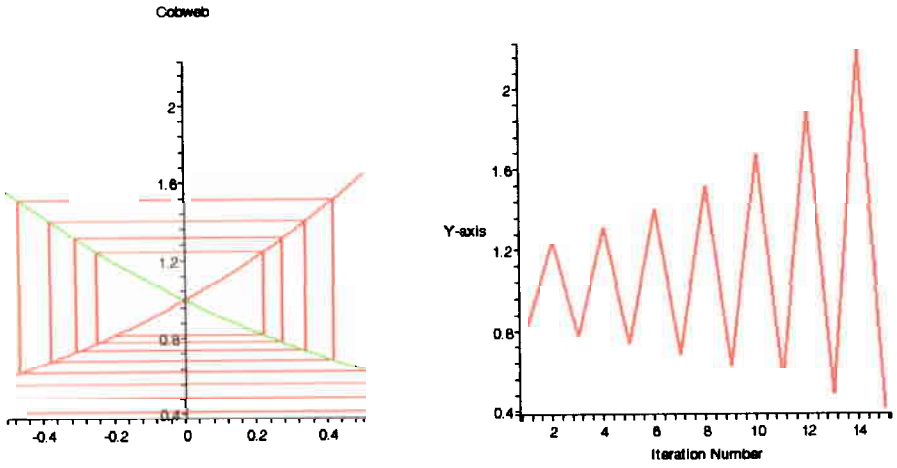

Fig. 12. X-axis is a function of T and the Y-axis is a measure of the reaction rate
ρ ~ strong coupling

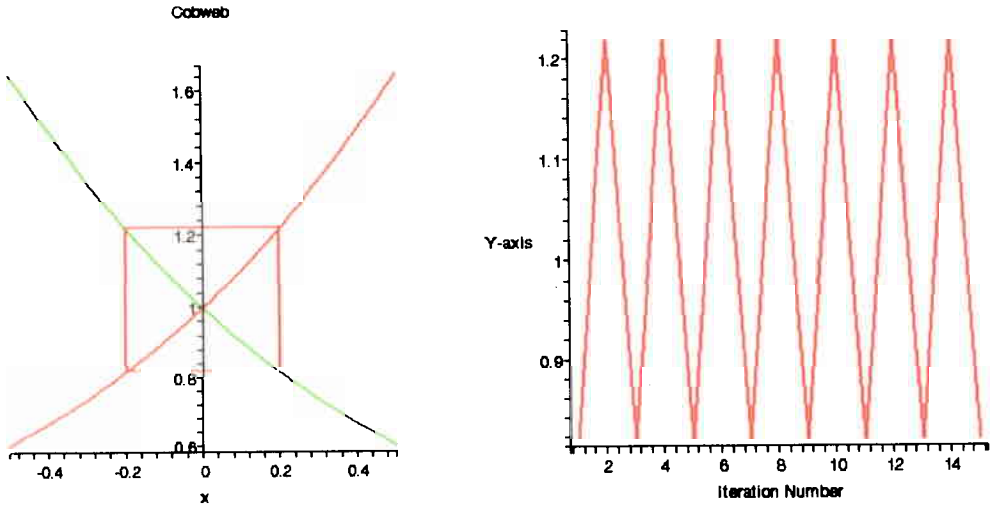

Fig. 13. X-axis is a function of T and the Y-axis is a measure of the reaction rate
ρ ~ medium coupling

A "limit cycle" appears around the equilibrium point. This represents a special condition where the system can develop a sustained oscillation that neither move toward or away from the equilibrium point.

These model predictions provided the guidance for searching for the effects experimentally. The chosen experimental allows the prediction of this model to be tested. The methodology for inducing the thermal runaway experimentally permitted the

number of constant current cycles used to induce the effect to be altered. Fifty cycles was found to be sufficient to induce the most severe effect. To establish a mild pretreatment, eight constant current cycles was applied to a new battery that was followed by the usual constant voltage charge. This resulted in the data shown in Figs. 14 and 15. This represents a condition corresponding to a loose coupling. The plots that follow include the response as a function of time and accumulated charge. This is the same data represented in two different ways.

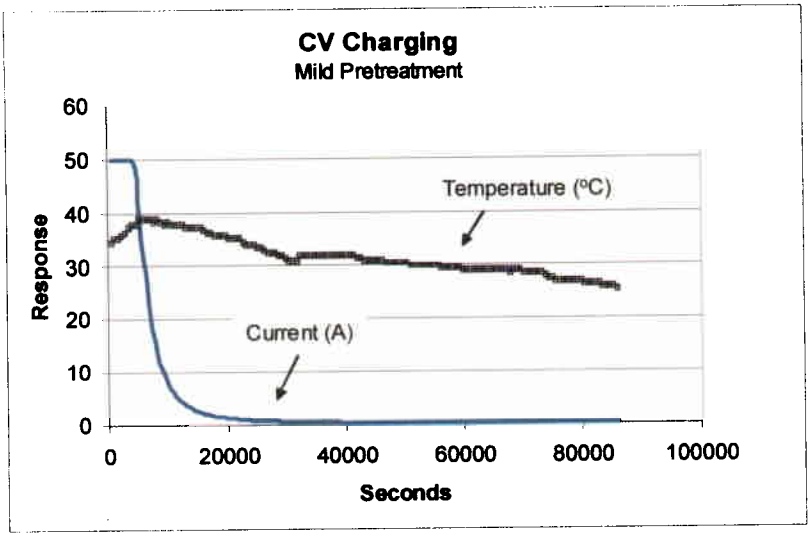

Fig. 14. Consequence of loose coupling shown as a function of time

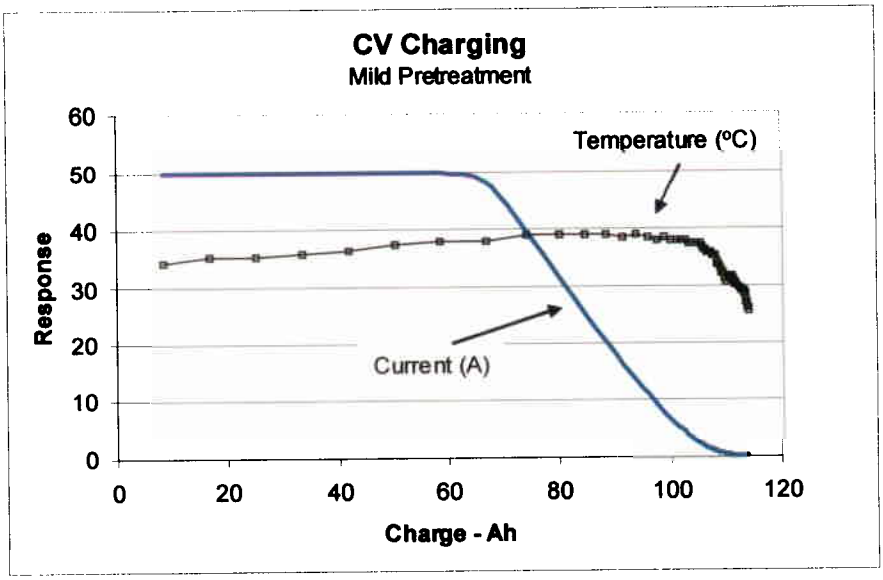

Fig. 15. Consequence of loose coupling shown as a function of charge

The system appears to have stabilized showing no apparent transition to a thermal runaway. A careful look at the data suggests a possible onset but the stabilization is evident.

An additional eight constant current cycles was applied to this same battery followed by the usual constant voltage charge. In this case, the effect of oscillation was observed. The data appears in Figs. 16 and 17

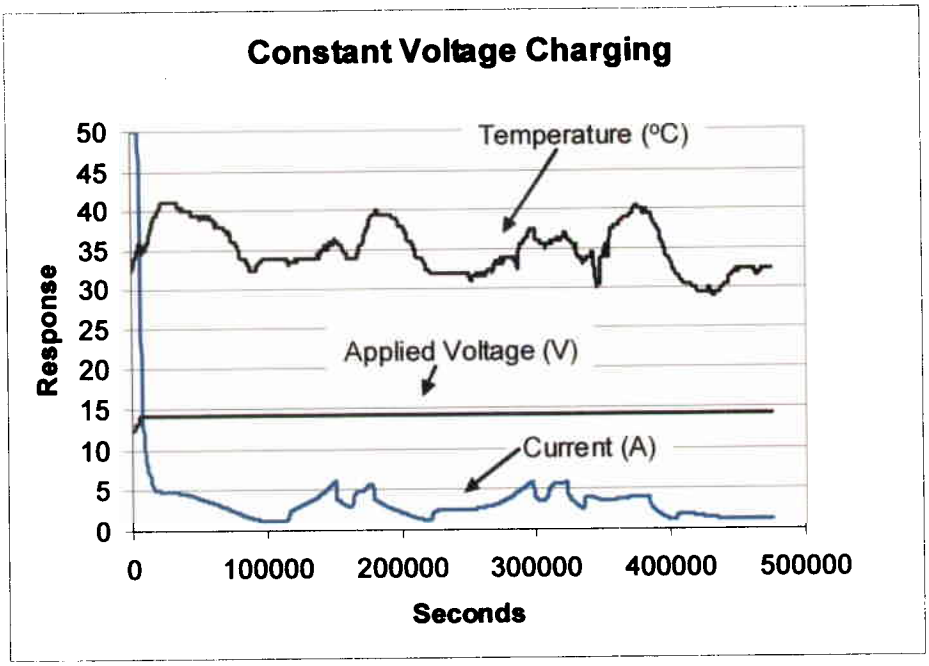

Fig. 16. Consequence of loose coupling shown as a function of time

The observed oscillatory behavior appears to be chaotic. It is consistent with the notion that it occurs when a special situation takes place consistent with an intermediate coupling between the electrolyte displacement by gas evolution and the return to the electrolyte to reduce the IR drop in the inter-cell gap.

Finally, a full fifty cycles was applied to drive the system into its worse case condition. This would represent the situation where a tight coupling would exist. The data is shown in Figs. 18 and 19.

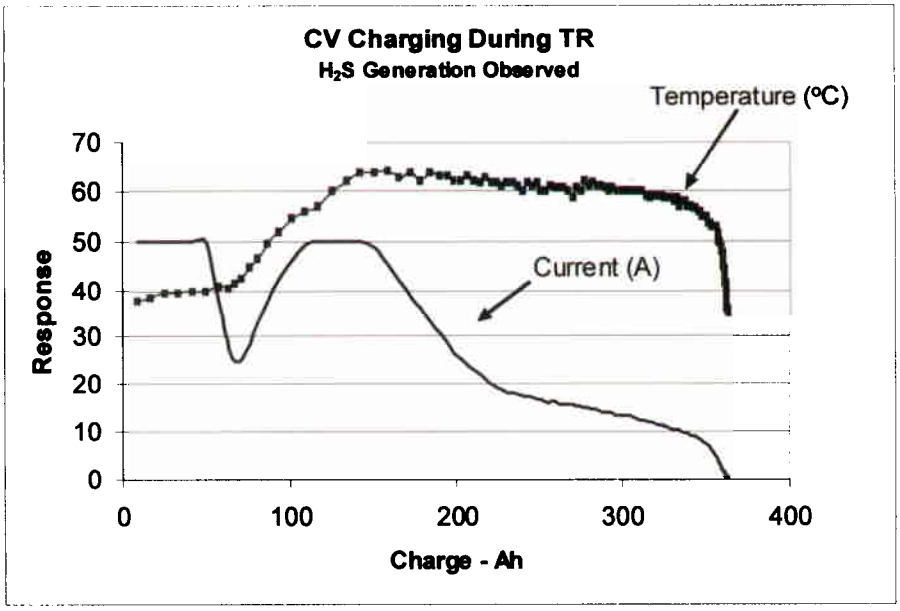

Fig. 19. Consequence of tight coupling shown as a function of accumulated charge

It is to be noted that the predicted reinforced oscillations did not occur. Since the uncontrolled oscillation represents the predicted behavior and it did not occur, the battery was examined closely to attempt an assessment as to why the ever increasing oscillations were absent. A close examination showed that all six vents on the battery were open with steam passing from the battery into the environment. As was mentioned earlier, the temperature measurement shown was the temperature of the negative electrode terminal with the heavy connectors and cabling attached. The temperature inside the battery is necessarily higher than the terminal temperature. The presence of the steam suggests that localized electrolyte boiling was taking place. Also, a very strong stench of hydrogen sulfide was being emitted from the battery. From these observations one can conclude that secondary processes take place acting to prevent a further rise in the battery temperature. The predicted reinforced oscillation appeared to have been damped by secondary processes.

The generation of hydrogen sulfide requires some additional remarks. The thermodynamic situation in a lead acid battery indicates that the reduction of sulfuric acid by lead is spontaneous. However, the kinetics of that process are very slow under normal operating conditions. Further, any trace amounts produced can be effectively scrubbed by the oxidizing power of the positive electrode. In the experiments performed, the high temperature produced in the interelectrode gap was sufficient to catalyze this kinetically slow process to a level where the hydrogen sulfide generation was very apparent the people standing in the immediate vicinity.

Conclusions

The cause of the thermal runaway appears to be associated with processes controlled by the separator. The approach to minimizing the TR effect would be to allow for a more efficient return of the displaced electrolyte into the inter cell gap. There is also a potential here for using proton conductive coatings on the fiber glass surface.

Temperature control could be used to place limits on the current allowed to pass into the cell. This would allow more time to permit electrolyte to reenter the inter-cell gap.

From the model presented above, it would follow that hydrogen generation from a negative limited charging condition could generate a thermal runaway. That is, the electrolyte displacement can be brought about by any gas generation process.

It is also noteworthy that the mechanism is independent of cell chemistry and should apply to cells having a constrained electrolyte that can be displaced by gas generated during charging.

Also, there exists a problem associated with the catalysis of other passive processes. H_2S production and in Li–ion cells, electrolyte conflagration are examples. The TR effect can serve to trigger an otherwise kinetically slow reaction.

References

[1] H.A. Catherino, F.F. Feres, and F. Trinidad, "Sulfation in Lead Acid Batteries," Journal of Power Sources, Volume 129, Issue 1, 15, April 2004, pp, 113-120.

[2] D. Pavlov, "Energy Balance of the closed oxygen cycle and process causing thermal runaway in valve-regulated lead/acid batteries," Journal of Power Sources, 64 (1997) 131-137.

[3] D. Pavlov and B. Monahov, Ext. Abstr., LABAT'96, 3-7 June 1996, Varna, Bulgaria.

[4] J.T. Sandefur, "Discrete Dynamical Modeling," Oxford University Press, New York, 1993.

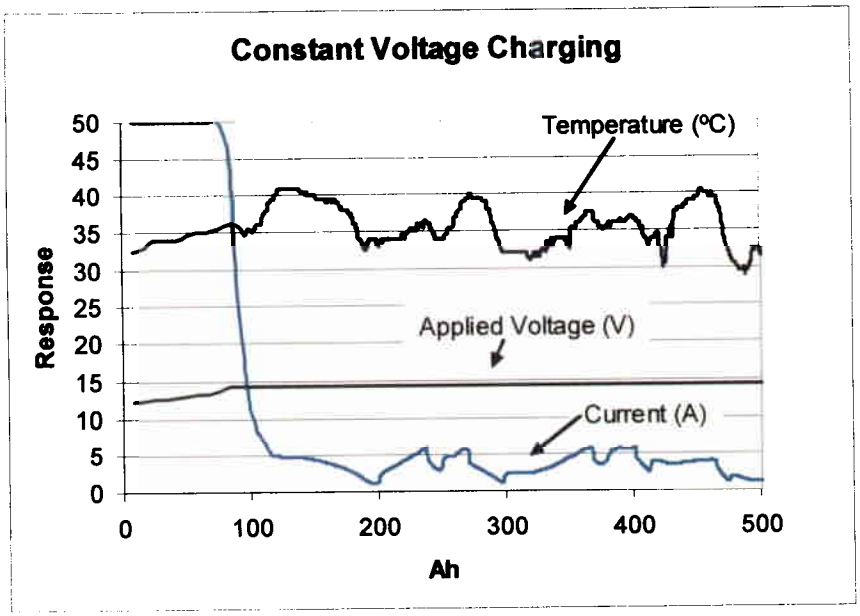

Fig. 17. Consequence of loose coupling shown as a function of accumulated charge

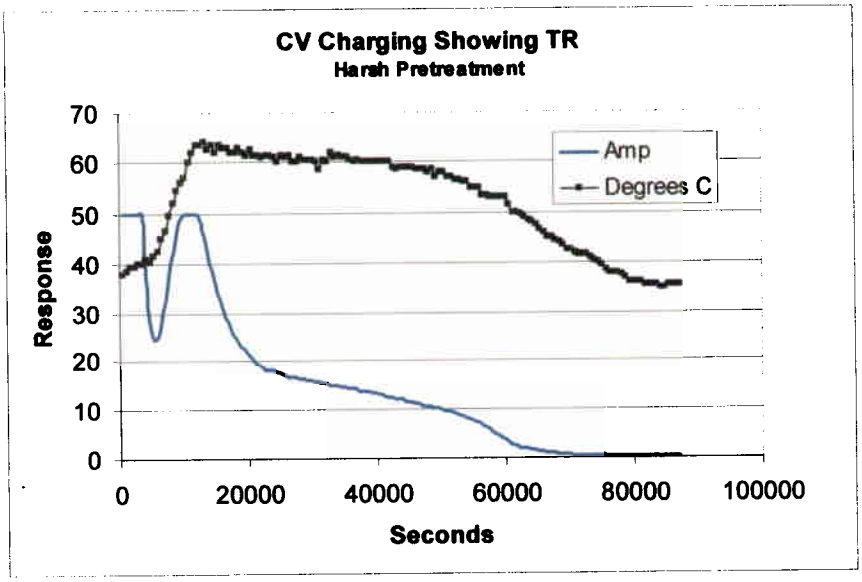

Fig. 18. Consequence of tight coupling shown as a function of time